Available online at www.sciencedirect.com

ScienceDirect

Procedia Manufacturing 15 (2018) 535–541

Procedia MANUFACTURING

www.elsevier.com/locate/procedia

17th International Conference on Metal Forming, Metal Forming 2018, 16-19 September 2018, Toyohashi, Japan

X-ray CT assisted damage identification in warm forging

Xian Zheng Lu, Luen Chow Chan*

Department of Industrial and Systems Engineering, The Hong Kong Polytechnic University, Hung Hom, Kowloon, Hong Kong

Abstract

This study aims to identify the 3-dimensional interactions of micro-voids evolution before and after warm-forging a typical titanium alloy component by employing a micro-focus X-ray CT system so as to achieve a more accurate micro-void location and distribution as critical data input for damage prediction in warm forging. A specific forging tool was designed for warm-forging the component. Serval local regions that represented different strain levels were established as representative volume element models for the Ti-6Al-4V preform, in which, the micro-void distributions were obtained directly from the X-ray CT images. Furthermore, the micro-void evolutions of the corresponding representative volume element models were analyzed from the forged component. Thus, the damage evolution, i.e., the variation of void volume fraction, in the warm forging process was identified.

Keywords: X-ray CT; Micro-voids; Damage; Warm forging; Representative volume element

1. Introduction

Forging is widely adopted in manufacturing various metallic components because of high production efficiency and enhanced material strength. Warm forging combines both technical advantages of hot forging and cold forging in terms of product quality and manufacturing costs [1]. It has the advantages of improving the material ductility and decreasing the material yield strength. Owing to the advantages of high strength to weight ratios, superior corrosion and fatigue resistance, titanium alloys are quite suitable for aerospace, marine and medical applications [2]. Due to high deformation resistance and spring back effect at room temperature, titanium alloys are often forged at elevated

* Corresponding author. Tel.: +852-2766-6634; fax: +852-2362-5267.
E-mail address: lc.chan@polyu.edu.hk

2351-9789 © 2018 The Authors. Published by Elsevier B.V.
Peer-review under responsibility of the scientific committee of the 17th International Conference on Metal Forming.
10.1016/j.promfg.2018.07.274

temperatures. This makes the material more readily and easily to deform and meanwhile conducive to stress releases. During forging process, the inherent micro-defects (e.g., micro-voids/cracks, inclusions, etc.) can be reduced or healed. However, some of the adjacent micro-defects may be aggregated and coalesced, which can lead eventually to damage accumulation and aggravation inside the component [3]. Therefore, it is very important to identify the damage evolution in forging process.

Traditional methods for damage identification are generally based on the examination of 2-dimensional sections of the corresponding components [4, 5]. Such testing procedures are destructive, time-consuming, and it is very difficult to locate the accurate cross-sections due to the complex shapes of forged components. In addition, processes that involve cutting and polishing during the preparation of specimens can destroy the micro-voids on the examined cross-sections [6, 7]. In view of this, X-ray computed tomography (CT) is a promising alternative technique that allows all-round visualization and identification of micro-voids in three dimensions during and after forging without any damage to the specimen material [8]. However, the application of non-destructive X-ray CT techniques for clearer damage identification in forging has rarely been studied.

In this study, the main objective was to identify the 3-dimensional interactions of micro-voids evolution before and after warm-forging a typical titanium alloy (Ti-6Al-4V, or equivalent) component by employing a high-resolution micro-focus X-ray CT system. A specific forging tool was designed for warm-forging the component. Serval local regions that represented different localized strain levels were established as geometrical representative volume element (RVE) models for the Ti-6Al-4V preform. Then the micro-void evolutions of the corresponding RVE models were analyzed from the forged component. Thus, the damage evolution, i.e., the variation of volume fraction of micro-voids, in the warm forging process was identified.

2. Experimental methods

2.1. Specimen preparation

Titanium alloy Ti-6Al-4V was selected as the specimen material for warm forging experiments. Typical warm forging temperature of 700 ºC was chosen for forging the Ti-6Al-4V component. The dimensions of the Ti-6Al-4V component for forging experiments is shown in Fig. 1(a). Such component could be produced by the closed-die forging process in one stroke. The preform was designed as a stepped cylinder as shown in Fig. 1(b). The parting lines of the die were set at the maximum cross section area; flashes were formed at the parting lines after the die cavity was filled fully, and the external flash thickness was set as 0.8mm.

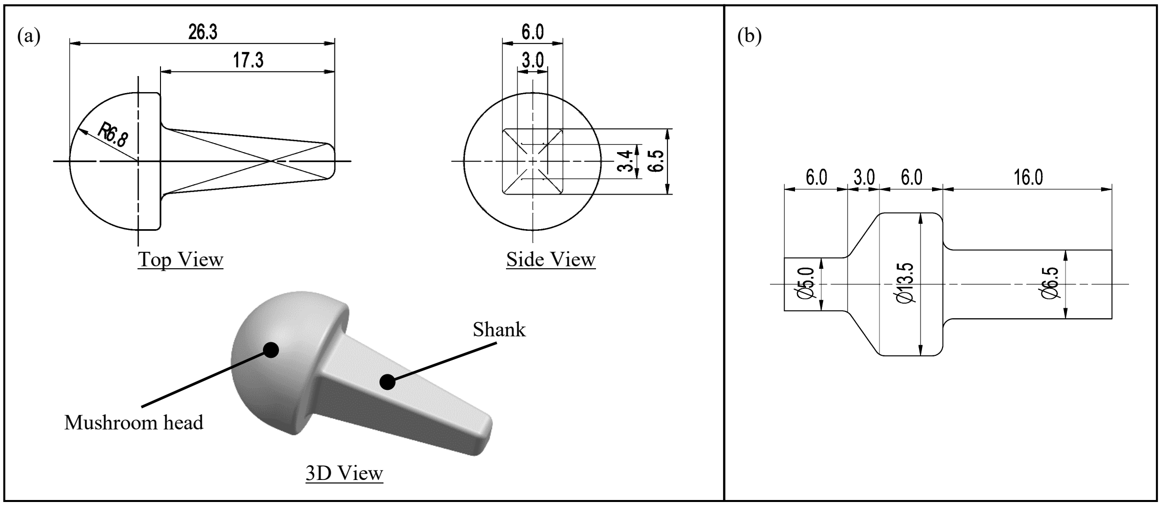

Fig. 1. (a) Configuration of Ti-6Al-4V component and (b) design and dimensions of pre-machined cast preform (all dimensions in mm).

2.2. Warm forging experiments

A specific forging tool, which mainly consists of upper and lower dies, heating and insulation devices, lift-up attachments and guide devices, was designed for warm-forging the Ti-6Al-4V component. It was installed on an experimental platform including a 160-ton AIDA mechanical press, a temperature controller, induction heating equipment, infrared thermometers, as shown in Fig. 2. Both upper and lower dies were heated by circular heaters to 250 °C, while the preform was heated by the induction heating equipment to the designated temperature (i.e., 700 °C) and then placed into the lower die for forging with a speed of 20 strokes per minute. The temperatures of the component and the dies were monitored continuously by the infrared thermal camera to ensure an accurate temperature control. Once forged, the component was taken out and quenched in water immediately to room temperature, thus to freeze the microstructure for the subsequent X-ray CT scanning.

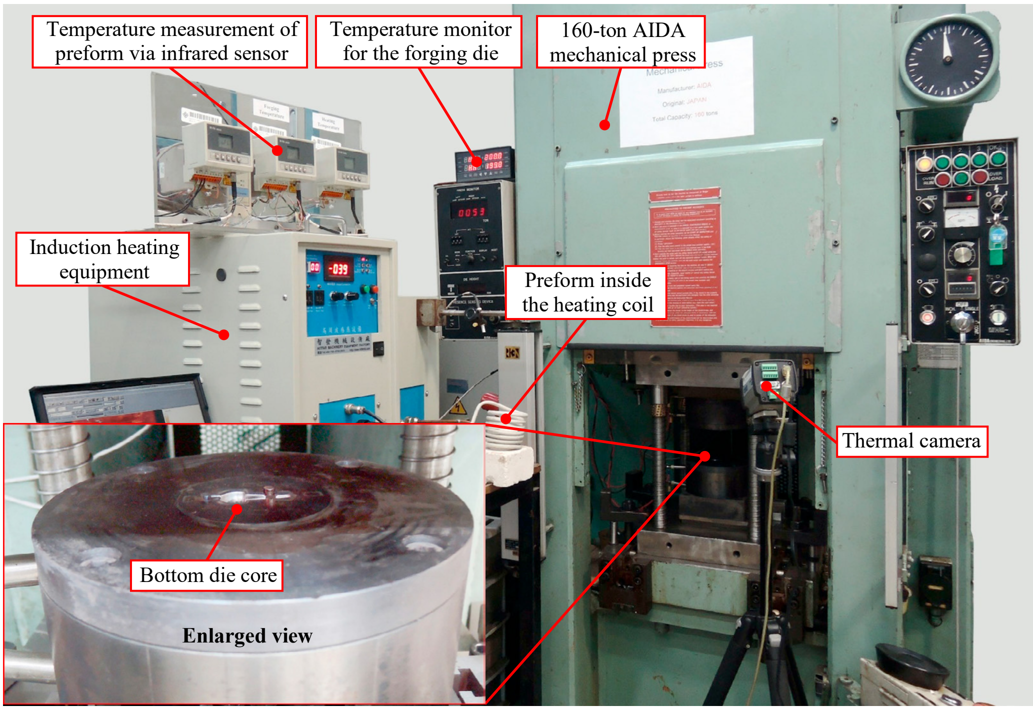

Fig. 2. Self-developed experimental platform for warm-forging Ti-6Al-4V component.

2.3. X-ray CT scanning

A micro-focus X-ray CT system YXLON FF35 CT, as shown in Fig. 3(a), was employed to detect the internal micro-void distributions of both the preform and forged component. The tube voltage and current were operated at 160 kV and 120 μA respectively for each scanning. 1440 projections were generated in 360° rotation, and the 3D volumetric CT data were generated using the in-house CERA reconstruction spooler. Then the reconstructed 2D and 3D CT images were visualized with VGStudio MAX 2.2. The comparison of relative pixel intensity values was adopted to separate the background and material in the CT images. The defect detection module in VGStudio was used to defect micro-voids from the volumetric CT data. Thus, information like size, number, spatial location, compactness, and sphericity of the micro-voids could be obtained. The 3D CT images with internal micro-voids of the preform are shown in Fig. 3(b). The voxel size of the CT image is 11.5 μm, which is high enough for void detection in the metallic materials [9]. It should be noted that the CT images were displayed semi-transparently to better reveal the distribution of internal micro-voids; the material is represented in grey and the micro-voids are represented in other colors.

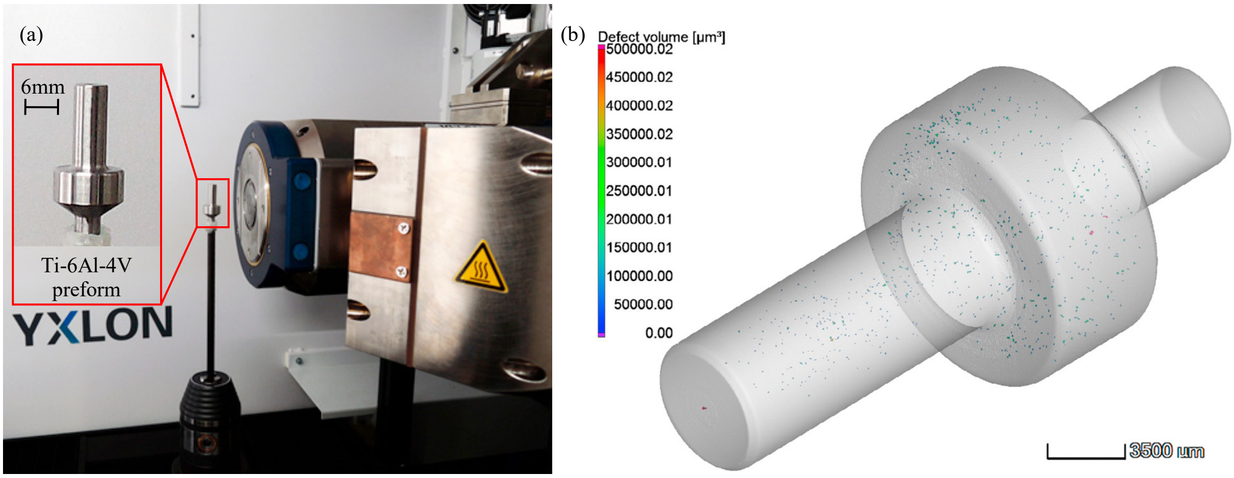

Fig. 3. (a) X-ray CT scanning of preform by YXLON FF35 CT system and (b) 3D CT images with internal micro-voids of preform.

3. Results and discussions

3.1. Construction of RVE models for Ti-6Al-4V preform

The quantitative analysis of the micro-voids for the Ti-6Al-4V preform from Fig. 3(b) showed that the sizes of the micro-voids ranged from 23.4 μm to 67.0 μm with an average size of 33.3 μm, and most of the micro-voids (approx. 66.0%) were sized between 28.8 μm and 36.7 μm. Since a large number of micro-voids were detected with random distribution and irregular shapes, it is very difficult to model all the micro-voids accurately and carry out the numerical prediction within a reasonable computational time. Therefore, several representative local regions of the preform were constructed as representative volume element (RVE) models to study the damage initiation and evolution during the warm forging process. The defect detection capabilities of the CT system and the application of an advanced segmentation algorithm ensured that the micro-voids inside the specimen can be identified accurately [10], which reduced the statistical error of the experimental procedure.

It is known that the stress triaxiality has a great influence on the onset and evolution of damage in ductile materials, which can be analysed experimentally through a series of tests including tensile (un-notched and notched specimens) and shear testing [11]. Since this study just focused on the warm forging process, such tests were not carried out. The varied stress distributions in different regions of the forged component enabled us to analyse the damage evolution at different strain conditions in one forging process. Thus, five typical local strain regions that represent different von Mises strain levels (i.e., 0.026, 0.111, 0.149, 0.359 and 0.691) were selected according to the predicted strain distribution of the forged component, as shown in Fig. 4, whereas the forged component was cut in half along the XY plane to better demonstrate its internal strain distribution. Details about the FE simulation conditions can be referred to our published work [10]. The void volume fraction strongly depends on the size of RVE. On the one hand, if the edge size of RVE is too small, there may be no micro-void included; on the other hand, if the edge size of RVE is too large, the strain/stress may vary a lot, which would result in the RVE cannot represent the damage under a specific strain level. Therefore, RVE models with side length of 1.0 mm were constructed from the preform in this study, as shown in Fig. 5. The void volume fraction of each RVE model was calculated, i.e., the total volume of micro-voids inside the RVE divided by the volume of RVE.

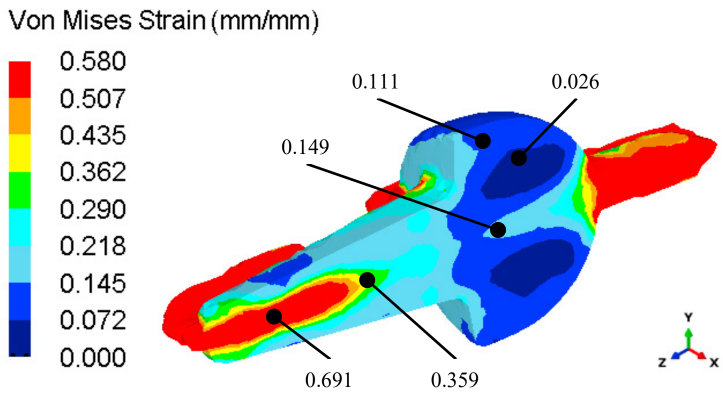

Fig. 4. Typical local strain regions of forged Ti-6Al-4V component.

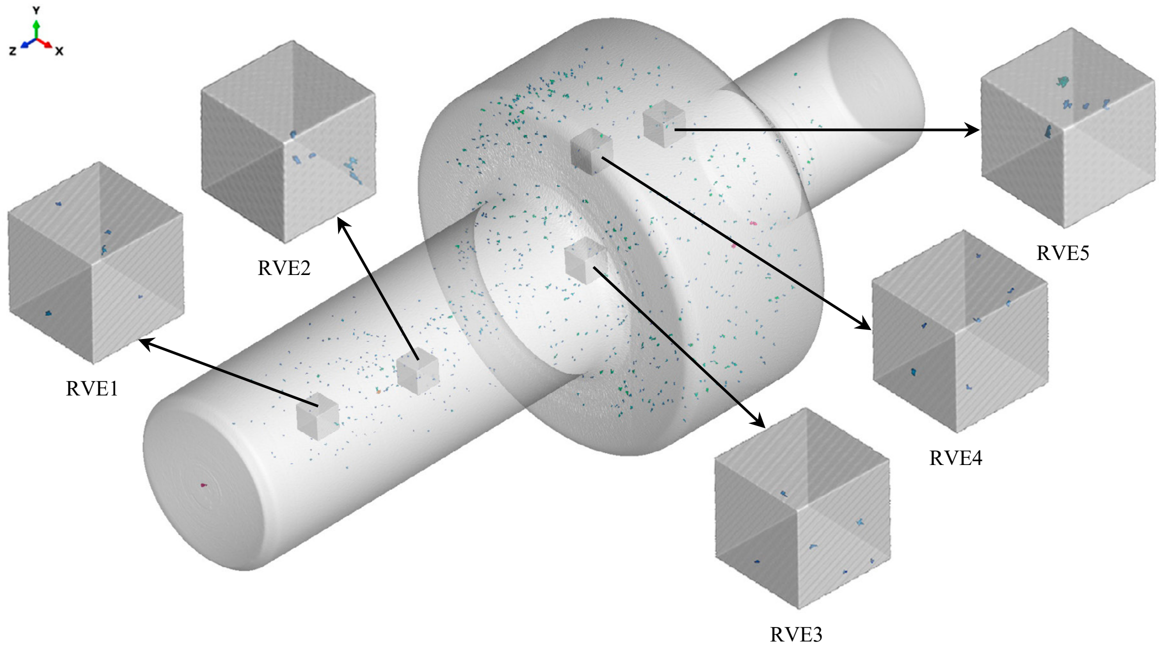

Fig. 5. RVE models (1.0 mm in side length) constructed after CT scan of Ti-6Al-4V preform before forging.

3.2. Damage evolutions of RVE models

The damage evolutions of the RVE models at different strain levels were analyzed. The forged component and its 3D CT images are shown in Fig. 6. The initial and final void volume fractions of these five RVE models are shown in Fig. 7(a). It can be seen that the initial void volume fractions of these RVE models were not the same, i.e., varied from 0.000154 to 0.000212, indicating the micro-voids were not uniformly distributed inside the preform. The forged component showed that the void volume fractions of RVE models under compression (i.e., RVE1, RVE2, RVE3) were increased very slowly. However, the void volume fraction under tension increased significantly, e.g., from 0.000191 to 0.00136 for RVE4. This was due to the shank of the specimen being compressed while part of the mushroom head being stretched (e.g., RVE4 and REV5) to form a sphere during warm forging. Ductile damage is most common in metallic materials under plastic deformation conditions, which is basically caused by the initiation and evolution of micro-cracks/voids [12-14]. According to continuum damage mechanics [15], the feature volume of the i_{th} micro-void in the RVE can be assumed as V_i, and the total number of micro-voids is N, then the total volume of micro-voids can be given as,

$$V = \sum_{i}^{N} V_i \quad (1)$$

Thus, the damage D can be defined directly as the volume fraction of micro-voids in the RVE, i.e.,

$$D = \frac{V}{V_{\mathrm{RVE}}}, \quad (2)$$

where V_{RVE} is the volume the RVE. It can be seen that the damage D is bounded by 0 and 1, $D = 0$ means undamaged material, while $D = 1$ indicates complete failure of the material. The changing of void volume fraction can be regarded as the damage evolution in the forging process, hence, the damage evolution at different strain levels was obtained, as shown in Fig. 7(b). Results showed that the damage evolved very slowly under compressive deformation, while it grew quickly under tensile deformation.

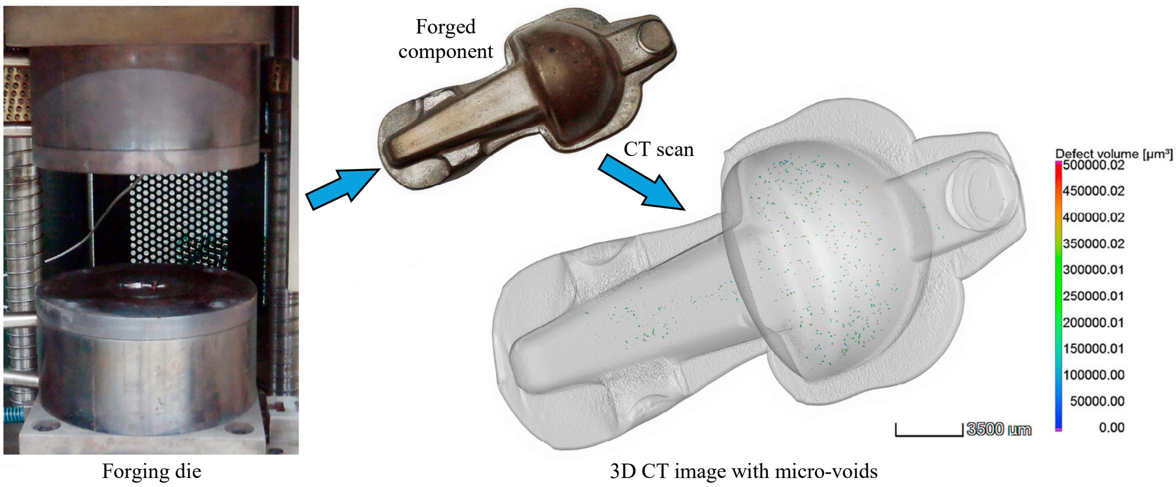

Fig. 6. Forging die and forged Ti-6Al-4V component together with its detected micro-voids after 3D CT scanning.

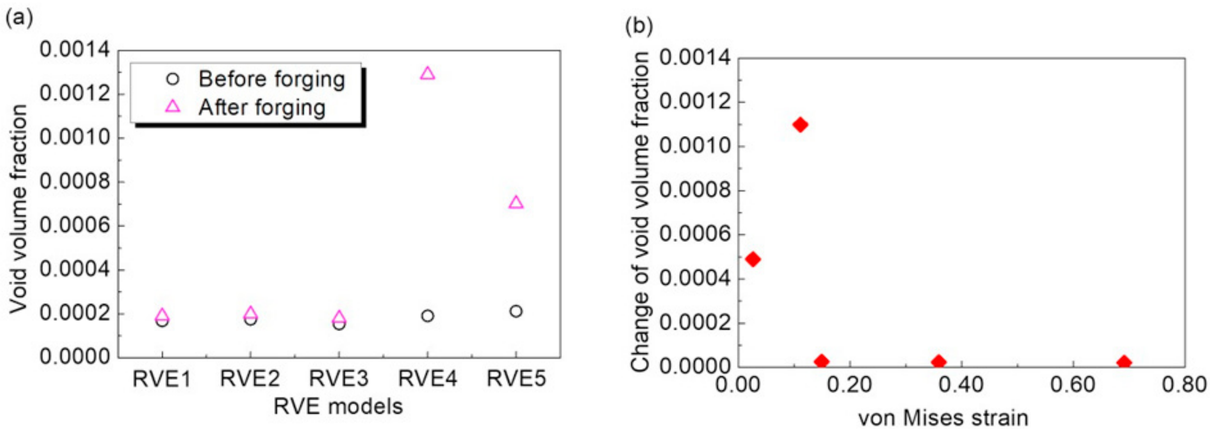

Fig. 7. (a) Initial and final void volume fractions of RVE models and (b) damage evolution at different strain levels.

4. Conclusions

In this study, 3-dimensional micro-voids evolution during and after warm-forging a Ti-6Al-4V component was identified by employing a high-resolution micro-focus X-ray CT system. Quantitative analysis of the micro-voids for the preform showed that the sizes of the micro-voids ranged from 23.4 μm to 67.0 μm with an average size of 33.3 μm, and most of the micro-voids were sized between 28.8 μm and 36.7 μm. A specific forging tool was designed for warm-forging the component. Serval representative local regions that represented different localized strain levels were established as RVE models for the Ti-6Al-4V preform. Results showed that the initial void volume fraction of these RVE models were not the same, i.e., varied from 0.000154 to 0.000191, indicating the micro-voids were not uniformly distributed inside the preform. CT scanning results of the forged component showed that the void volume fractions of RVE models under compression increased very slowly. However, the void volume fraction under tension increased significant to 0.00136 for RVE4. Further analysis revealed that the damage evolved very slowly under compressive deformation, while it grew quickly under tensile deformation.

Acknowledgements

The work described in this paper was partially supported by grants from the Research Committee of The Hong Kong Polytechnic University (student account code RTBN and project code G-YL64), Large Equipment Fund of the Hong Kong Polytechnic University (Project No. DD6X), and the grant from the Research Grants Council of the Hong Kong Special Administrative Region, China (Project No. PolyU 511511).

References

[1] S. Sheljaskov, Current level of development of warm forging technology, Journal of Materials Processing Technology, 46 (1994) 3–18.
[2] C. Leyens, M. Peters, (Eds.), Titanium and titanium alloys: fundamentals and applications, John Wiley & Sons, (2003).
[3] T. Ishikawa, N. Yukawa, Y. Yoshida, Y. Tozawa, Analytical approach to elimination of surface micro-defects in forging, CIRP Annals-Manufacturing Technology, 54 (2005) 249–252.
[4] I. Gitman, H. Askes, L. Sluys, Representative volume: existence and size determination, Engineering Fracture Mechanics, 74 (2007) 2518–2534.
[5] P.J. Zhao, Z.H. Chen, C.F. Dong, Failure analysis based on microvoids damage model for DP600 steel on in-situ tensile tests, Engineering Fracture Mechanics, 154 (2016) 152–168.
[6] M. Kaye, C. Puncreobutr, P.D. Lee, D.S. Balint, T. Connolley, D. Farrugia, J. Lin, A new parameter for modelling three-dimensional damage evolution validated by synchrotron tomography, Acta Materialia, 61 (2013) 7616–7623.
[7] L. Babout, E. Maire, J.Y. Buffière, R. Fougeres, Characterization by X-ray computed tomography of decohesion, porosity growth and coalescence in model metal matrix composites, Acta Materialia, 49 (2001) 2055–2063.
[8] J. Hsieh, Computed tomography: principles, design, artifacts, and recent advances, SPIE Bellingham, WA, (2009).
[9] R.D.K. Misra, X.L. Wan, V.S.A. Challa, M.C. Somani, L.E. Murr, Relationship of grain size and deformation mechanism to the fracture behavior in high strength–high ductility nanostructured austenitic stainless steel, Material Science and Engineering: A, 626 (2015) 41–50.
[10] X.Z. Lu, L.C. Chan, Micromechanics-based damage model for failure prediction in cold forming, Materials Science and Engineering: A, 690 (2017) 120–131.
[11] M. Brünig, O. Chyra, D. Albrecht, L. Driemeier, M. Alves, A ductile damage criterion at various stress triaxialities, International Journal of Plasticity, 24 (2008) 1731–1755.
[12] V.N.V. Do, The behavior of ductile damage model on steel structure failure, Procedia Engineering, 142 (2016) 26–33.
[13] T.S. Cao, Models for ductile damage and fracture prediction in cold bulk metal forming processes: a review, International Journal of Material Forming, 10 (2017) 139–171.
[14] X.Z. Lu, L.C. Chan, Micro-voids quantification for damage prediction in warm forging of biocompatible alloys using 3D X-ray CT and RVE approach, Journal of Materials Processing Technology, 258 (2018) 116–127.
[15] J. Lemaitre, A course on damage mechanics, Springer Science & Business Media, (2012).